

# X-ray Powder Diffraction Structure Reinvestigation of the $\alpha$ and $\beta$ Forms of Cobalt Phthalocyanine and Kinetics of the $\alpha \rightarrow \beta$ Phase Transition

Paolo Ballirano,<sup>†</sup> Ruggero Caminiti,<sup>\*,‡</sup> Claudio Ercolani,<sup>§</sup> Adriana Maras,<sup>||</sup> and Maria Antonietta Orrù<sup>§</sup>

Contribution from the Dipartimento di Chimica, INFM Istituto Nazionale di Fisica della Materia, Università degli studi di Roma "La Sapienza", P.le A. Moro 5, 00185 Roma, Italy, Dipartimento di Chimica, Università degli studi di Roma "La Sapienza", P.le A. Moro 5, 00185 Roma, Italy, and Dipartimento di Scienze della Terra, Università degli studi di Roma "La Sapienza", P.le A. Moro 5, 00185 Roma, Italy

Received November 5, 1997

**Abstract:** The structures of the acid-paste-prepared  $\alpha$ -form of cobalt phthalocyanine ( $\alpha$ -PcCo) and of its corresponding  $\beta$ -form ( $\beta$ -PcCo) have been refined through X-ray powder diffraction using the Rietveld method. The  $\alpha$ -polymorph is triclinic, space group  $P\bar{1}$ , cell parameters  $a = 12.090(8)$  Å,  $b = 3.754(2)$  Å,  $c = 12.800(9)$  Å,  $\alpha = 88.96(6)^\circ$ ,  $\beta = 90.97(6)^\circ$ ,  $\gamma = 95.09(7)^\circ$ , and  $Z = 1$ ; the  $\beta$ -form is monoclinic, space group  $P2_1/a$ , cell parameters  $a = 14.5982(9)$  Å,  $b = 4.7937(3)$  Å,  $c = 19.4348(11)$  Å,  $\beta = 120.782(3)^\circ$ , and  $Z = 2$ .  $\alpha$ -PcCo consists of columnar arranged molecules, those of adjacent columns being aligned parallel to each other, whereas a nearly perpendicular arrangement is present in  $\beta$ -PcCo.  $\alpha$ -PcCo also differs from the  $\alpha$ -forms of PcH<sub>2</sub> and PcPt in which an angle of ca.  $125^\circ$  is observed between molecules of closely contacting chains. From the refined peak-profile parameters of the powder pattern a crystallite size of  $\sim 150$  Å has been estimated for  $\alpha$ -PcCo, a value approaching that of nanocompounds. The isothermal  $\alpha \rightarrow \beta$  phase transition has been followed in-situ real-time by means of EDXD at two different temperatures, 152 and 250 °C. Calorimetric data indicate two different behaviors of the rate constant in the temperature ranges 182.5–220 and 220–270 °C leading to values of the empirical activation energy,  $E_a$ , of 36.6(16) and 14.8(9) kcal/mol, respectively. However the various DSC runs lead to values of the phenomenological  $n$  parameter in the range 2.34–2.68 (indicating an isokinetic two-dimensional growth). According to the combined EDXD and DSC data a three-step model for the  $\alpha \rightarrow \beta$  PcCo phase transition may be proposed: (1) disordering of adjacent layers of PcCo molecules from their original  $\alpha$ -type arrangement; (2) crystallization of the  $\beta$ -form from the disordered phase through rearrangement of the layers of the phthalocyanine units; (3) crystal growth of the  $\beta$ -phase from the nuclei to an average particle size of  $\sim 2500$  Å, as indicated by the fitted peak-profile parameters. No evidence of the occurrence of intermediate ordered phases was observed.

## Introduction

Phthalocyanine compounds of formula PcM (Pc = phthalocyaninato anion C<sub>32</sub>H<sub>16</sub>N<sub>8</sub><sup>2-</sup>, M = H<sub>2</sub> or a bivalent metal) have been known to exist in different solid modifications ( $\alpha$ ,  $\beta$ ,  $\gamma$ ,  $\delta$ ,  $\epsilon$ ,  $\chi$ ). The best-characterized are the  $\beta$ <sup>1–4</sup> and  $\alpha$  polymorphs,<sup>5,6</sup> in some cases elucidated by single-crystal X-ray work. However different  $\alpha$ -forms have been identified in the literature, often depending on the different preparation method used (see for instance PcZn<sup>7</sup>). Nevertheless, there is a considerable confusion

about the structural properties and the nomenclature of many polymorphs of PcM as indicated by the description of as many as three different  $\alpha$ -forms of PcZn.<sup>7</sup>

The usually commercialized  $\beta$  solid modification can be changed into the  $\alpha$ -form either by precipitation from solutions of the metal phthalocyanine in concentrated (96%) H<sub>2</sub>SO<sub>4</sub> (acid-paste method) or by sublimation under vacuum and condensation of the vaporized metal phthalocyanine onto a plate maintained at low temperature (100 °C or lower). The  $\alpha$  form can be converted into the  $\beta$  form by heating the solid material under vacuum for a time long enough depending on the temperature used for the conversion. In a classical work<sup>8</sup> the conversion of the  $\alpha$  form, obtained by the sublimation method, into the  $\beta$  form, a criterion was given for the identification of the two different forms by their different IR spectra.

Despite the assumed isomorphism among some  $\alpha$ -PcM, close inspection of the reported interplanar spacings and relative intensities (Table 1) reveal significant discrepancies among the various phthalocyanines. Particularly interesting are the differences revealed by the two data sets of PcCu samples prepared by the

<sup>†</sup> Corso Duca di Genova 147, Roma, I-00121.

<sup>‡</sup> Dipartimento di Chimica, Istituto Nazionale di Fisica della Materia.

<sup>§</sup> Dipartimento di Chimica.

<sup>||</sup> Dipartimento di Scienze della Terra.

\* To whom correspondence should be addressed. E-Mail: r.caminiti@caspur.it.

(1) Kirner, J. F.; Dow, W.; Scheidt, W. R. *Inorg. Chem.* **1976**, *15*, 1685.

(2) Scheidt, W. R.; Dow, W. *J. Am. Chem. Soc.* **1977**, *99*, 1101.

(3) Mason, R.; Williams, G. A.; Fielding, P. E. *J. Chem. Soc., Dalton Trans.* **1979**, 676.

(4) Kubiak, R.; Janczak, J. *J. Alloys Compd.* **1992**, *190*, 117.

(5) Brown, C. J. *J. Chem. Soc. A* **1968**, 2494.

(6) Kubiak, R.; Janczak, J. *J. Alloys Compd.* **1992**, *190*, 121.

(7) Kobayashi, T.; Fujiyoshi, Y.; Iwatsu, F.; Uyeda, N. *Acta Crystallogr.* **1981**, *A37*, 692.

(8) Sidorov, A. N.; Kotlyar, I. P. *Opt. Spekt.* **1961**, *11*, 175.

**Table 1.** Interplanar Spacings and Relative Intensities of  $\alpha$ -PcM Reported by Various Authors

				Ashida et al. (1966)									
PcCu <sup>a</sup>		PcCu <sup>b</sup>		PcCo <sup>a</sup>		PcFe <sup>a</sup>		PcH <sub>2</sub> <sup>a</sup>		PcNi <sup>a</sup>		PcPt <sup>a</sup>	
<i>d</i> (Å)	<i>I</i> / <i>I</i> <sub>0</sub>	<i>d</i> (Å)	<i>I</i> / <i>I</i> <sub>0</sub>	<i>d</i> (Å)	<i>I</i> / <i>I</i> <sub>0</sub>	<i>d</i> (Å)	<i>I</i> / <i>I</i> <sub>0</sub>	<i>d</i> (Å)	<i>I</i> / <i>I</i> <sub>0</sub>	<i>d</i> (Å)	<i>I</i> / <i>I</i> <sub>0</sub>	<i>d</i> (Å)	<i>I</i> / <i>I</i> <sub>0</sub>
13.01	vs	12.96	vs	12.9	vs	13.1	vs	13.1	s	13.06	s	13.12	vs
11.90	s	12.05	vs	12.6	vs	12.5	vs	11.9	vs	12.12	vs	11.99	s
		8.817	m							8.54	w	9.14	w
6.48	s			6.47	s	6.55	s	6.56	s	6.56	m	8.43	w
				6.27	s							6.56	s
5.99	m					6.05	s	5.96	vs	6.06	s	5.96	m
5.64	w	5.671	w							5.68	m	5.61	m
		5.479	w							5.34	w		
4.32	m			4.32	m	4.34	m	4.35	m	4.36	m	4.62	w
				4.18	w	4.13	vw					4.37	w
4.01	w	4.068	w					3.97	w	4.05	m	4.19	vw
3.77	w			3.72	m	3.72	m	3.77	m	3.77	m	4.01	vw
3.68	m	3.704	m	3.66	w			3.73	w	3.68	m	3.78	m
3.59	m	3.560	m	3.56	w	3.58	m	3.61	s	3.56	w	3.62	m
						3.49	s						
3.40	m			3.43	m	3.43	vw	3.42	s			3.41	m
						3.39	vw						
3.33	m	3.338	m	3.36	vw							3.28	vw
3.22	m	3.233	m	3.25	vw	3.25	vw	3.25	vw	3.24	s	3.21	vw
						3.17	w	3.20	m	3.19	s		
						3.07	w			3.05	vw	3.03	m
2.93	w					2.95	vw	2.97	m			2.99	vw
						2.89	m	2.84	w	2.82	w	2.95	m
												2.86	vw
Ercolani et al. (1967)				Kobayashi et al. (1968)				Iwatsu (1985)					
PcCo <sup>b</sup>		PcCr <sup>b</sup>		PcZn <sup>a</sup>		PcZn <sup>a</sup>		PcZn <sup>a</sup>		PcZn <sup>a</sup>		PcZn <sup>a</sup>	
<i>d</i> (Å)	<i>I</i> / <i>I</i> <sub>0</sub>	<i>d</i> (Å)	<i>I</i> / <i>I</i> <sub>0</sub>	<i>d</i> (Å)	<i>I</i> / <i>I</i> <sub>0</sub>	<i>d</i> (Å)	<i>I</i> / <i>I</i> <sub>0</sub>	<i>d</i> (Å)	<i>I</i> / <i>I</i> <sub>0</sub>	<i>d</i> (Å)	<i>I</i> / <i>I</i> <sub>0</sub>	<i>d</i> (Å)	<i>I</i> / <i>I</i> <sub>0</sub>
12.40	vs	12.55	vs	12.99	vs	12.99	vs	12.99	vs	12.99	vs	12.99	vs
				12.30	s	12.30	s	12.30	s	12.30	s	12.30	s
				10.10	w	10.10	w						
				9.54	m	9.54	m						
8.79	m	8.93	m	8.90	w	8.90	w	8.90	w	8.90	w	8.90	w
		6.30	w										
5.60	m	5.66	s	5.70	m	5.70	m	5.70	m	5.70	m	5.70	m
				5.51	m	5.51	m	5.51	m	5.51	m	5.51	m
				4.28	w	4.28	w	4.28	w	4.28	w	4.28	w
		3.99	vw										
3.69	w	3.71	m										
3.56	w	3.56	s										
				3.46	s	3.46	s	3.46	s	3.46	s	3.46	s
				3.42	s	3.42	s	3.42	s	3.42	s	3.42	s
				3.40	s	3.40	s	3.40	s	3.40	s	3.40	s
3.34	m	3.29	m	3.23	m	3.23	m	3.23	m	3.23	m	3.23	m
3.20	s	3.16	vw										
		3.06	w										
		2.97	w										
2.82	vvw	2.84	vw	2.92	m	2.92	m	2.92	m	2.92	m	2.92	m

<sup>a</sup> Synthesized by sublimation under vacuum. <sup>b</sup> Synthesized from the so-called acid-paste method (precipitation from solutions of PcM in concentrated H<sub>2</sub>SO<sub>4</sub>).

above-proposed procedures. PcCu synthesized by sublimation shows three relatively strong reflections at 6.48, 5.99, and 4.32 Å that are not present into the corresponding diffraction pattern of acid-paste PcCu. On the other side, acid-paste PcCu shows an intense reflection, corresponding to an interplanar spacing of 8.82 Å, that is not present into the pattern of sublimated PcCu. Similar discrepancies may be observed also for PcCo.

In the present work the attention has been focused on  $\alpha$ -PcCo and in particular on its structural features and the kinetics of the  $\alpha \rightarrow \beta$  phase transition. Among the various phthalocyanines,  $\alpha$ -PcCo is one of the less studied from the structural point of view. In fact, only qualitative information is known for  $\alpha$ -PcCo<sup>9,10</sup> whereas the  $\beta$  polymorph has been investigated in

detail through single-crystal X-ray<sup>3</sup> and neutron<sup>11</sup> diffraction. No single crystals of adequate dimensions of  $\alpha$ -PcCo have been grown so far, and this fact has prevented structural study through conventional techniques. The problem has been faced in the present contribution by the use of the Rietveld refinement of powder data,<sup>12,13</sup> recently proven to be very successful in solving the structure of organic materials not available as single

(9) Ashida, M.; Uyeda, N.; Suito, E. *Bull. Chem. Soc. Jpn.* **1966**, *39*, 2616.

(10) Ercolani, C.; Neri, C.; Porta, P. *Inorg. Chim. Acta* **1967**, *1*, 415.

(11) Williams, G. A.; Figgis, B. N.; Mason, R.; Mason, S. A.; Fielding, P. E. *J. Chem. Soc., Dalton Trans.* **1980**, 1688.

(12) Rietveld, H. *Acta Crystallogr.* **1967**, *22*, 151.

(13) Rietveld, H. *J. Appl. Crystallogr.* **1969**, *2*, 65.

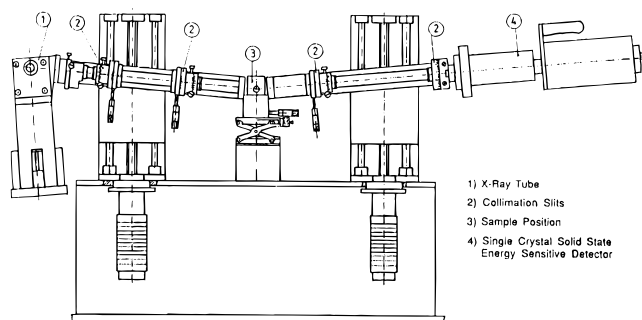


**Figure 1.** Schematic view of the prototype of the energy dispersive diffractometer.

crystals.<sup>14</sup> The  $\alpha \rightarrow \beta$  PcCo phase transition has been studied by the energy dispersive X-ray diffraction (EDXD) method, particularly useful for low crystallinity or amorphous materials for which traditional X-ray diffraction techniques may be applied with extreme difficulty.<sup>15–17</sup> The data obtained through EDXD have been complemented with a detailed differential scanning calorimetry (DSC) study in order to derive the thermodynamical and kinetic parameters and a more complete description of the phase transition.

### Experimental Section

PcCo was an Eastman Kodak product that was purified and obtained in the  $\beta$  crystalline modification ( $\beta$ -PcCo) by sublimation under vacuum (400–450 °C,  $10^{-2}$  mmHg). The  $\alpha$  polymorph was obtained by dissolving  $\beta$ -PcCo in concentrated  $\text{H}_2\text{SO}_4$  (96%) followed by reprecipitation by pouring the solution into iced water. The separated solid was washed abundantly with water and dried under vacuum.

Room-temperature powder diffraction data for structure refinement/solution have been obtained with a conventional Seifert MZ IV  $\theta/2\theta$  Bragg–Brentano automated diffractometer. Powder diffraction patterns were collected in step-scan mode in the  $3\text{--}159^\circ$   $2\theta$  range with a step-size of  $0.02^\circ$  in  $2\theta$  and 6 s of counting time, using graphite-monochromatized Cu  $K\alpha$  radiation. The powders were loaded inside a 0.5-mm deep cavity of a conventional glass sample-holder and gently pressed with a glass slide in order to minimize preferred orientation.

The nonambient temperature X-ray data were collected with a prototype of an EDXD instrument.<sup>18,19</sup> In EDXD an incident polychromatic X-ray radiation is used and the diffracted beam is energy resolved by a solid-state detector located at a suitable scattering angle. The modulus of the scattering vector  $q$  (function of the energy of the photon  $E$  and the scattering angle  $\theta$ ) can be represented as

$$q(E, \theta) = 1.014E \sin \theta = \frac{4\pi(\sin \theta)}{\lambda} \quad (1)$$

where  $q$  is expressed in  $\text{\AA}^{-1}$ ,  $\lambda$  in  $\text{\AA}$ , and  $E$  in keV.

The instrument (Figure 1), operating in vertical  $\theta/\theta$  geometry, is equipped with an X-ray generator (W target), a collimating system, step motors, and a solid-state detector connected via an electronic chain to a multichannel analyzer. A thermostatic cell is placed at the common center of rotation of the diffractometer arms.<sup>16</sup> The X-ray source is a standard Seifert tube operating at 45 kV and 35 mA whose Bremsstrahlung radiation is used. The fluorescence L lines of W are in the 8–11

keV range and do not interfere with our measurements being outside the region of interest. The detecting system is composed of an EG&G liquid-nitrogen-cooled ultrapure Ge solid-state detector ORTEC 92X connected to a PC through ADCAM hardware. The collimating system consists of four adjustable W slits. Both X-ray tube and detector holding arms can rotate, with the aid of step motors, around their common center in order to reach the desired scattering angle (reproducibility  $> 0.001^\circ$  in  $2\theta$ ).

A particular value of the diffraction angle  $\theta$  was chosen in order to select a portion of the diffraction pattern where peaks of  $\alpha$ - and  $\beta$ -forms were easily recognized. A preliminary run on a conventional  $\theta/2\theta$  X-ray powder diffractometer indicated that the first part of the spectrum of the two polymorphs fulfills this requirement especially because at angle  $> 40^\circ$  in  $2\theta$  of Cu radiation the intensities of the  $\alpha$  form decrease drastically. According to these experimental problems a diffraction angle  $\theta$  of  $2.2^\circ$  was selected, corresponding to  $0.4 < q < 1.5 \text{ \AA}^{-1}$ .

Calorimetric data have been obtained on a power-compensated type of differential scanning calorimeter (Perkin-Elmer DSC-7) equipped with a Pt/Ir furnace. Prior the DSC runs temperature and heat of reaction were calibrated with indium standard. A constant sample weight of 5.2 mg was used to minimize the heat transfer effect of PcCo. All the measurements were carried out under  $\text{N}_2$  flow. A total of 20 different isothermal runs were collected in the temperature range 182.5–270 °C.

### Structure Determination/Refinement

The structure determination/refinement of the two samples of  $\alpha$ - and  $\beta$ -PcCo was carried out with the PC version of the crystal structure analysis package GSAS.<sup>20</sup> As initial structural parameters of the  $\beta$  phase we used those of the room-temperature refinement of PcCo.<sup>3</sup> Data were evaluated in the  $11.5\text{--}90^\circ$   $2\theta$  angular range in order to fully characterize the starting material. A total of 75 soft constraints on bond distances and angles were imposed (full list of soft constraints available from the authors upon request), initially with high statistical weight that was subsequently reduced during the refinement. This was done to avoid divergence or convergence toward false minima (for discussions on soft-constraints and Rietveld refinements see ref 21). Only four coefficients of the cosine Fourier series describing the background, along with the cell parameters, were allowed to vary. During the successive cycles the Gaussian  $\theta$ -independent parameter GW of the pseudo-Voigt function used to model the peak-shape<sup>22</sup> and the tan  $\theta$ -dependent Lorentzian parameter LY were released. At this point of the refinement the positional parameters of the various atoms, with an associated high damping factor, were freed along with the  $1/\cos \theta$  dependent Lorentzian parameter LX, a profile asymmetry parameter Asym, and a fifth background coefficient. Despite the fact that hydrogen atoms could not be located in difference Fourier maps, they were finally included to the refinement in position expected from reference data<sup>3</sup> and refined using 38 more soft constraints on bond distances and angles. In the final cycles isotropic displacement parameters for metal, nonmetal (C and N), and hydrogen atoms were also refined. The profile fitting smoothly converged to agreement indices<sup>23</sup>  $R_p = 0.073$ ,  $wR_p = 0.096$ ,  $\chi^2 = 1.69$ , and  $R_{\text{BRAGG}} = 0.130$ . A careful scrutiny of the difference plot did not indicate significant preferred orientation effects. An attempt to model the presence of texture by means of a generalized spherical-harmonic description<sup>24,25</sup> led to a small improvement of the fit as a result of a texture index  $J = 1.51$  ( $J = 1$  for an ideal “random powder”;  $J = \infty$  for a single crystal). Final agreement indices were  $R_p = 0.067$ ,  $wR_p = 0.089$ ,  $\chi^2 = 1.45$ , and  $R_{\text{BRAGG}} = 0.121$ .

(14) Ballirano, P.; Caminiti, R.; Coiro, V.; Mancini, G.; Maras, A.; Sadun, C. *Z. Krist.* **1998**, *213*, 123–129.

(15) Rossi Albertini, V.; Bencivenni, L.; Caminiti, R.; Cilloco, F.; Sadun, C. *J. Macromol. Sci.-Phys.* **1996**, *B35*, 199.

(16) Rossi Albertini, V.; Caminiti, R.; Cilloco, F.; Croce, F.; Sadun, C. *J. Macromol. Sci.-Phys.* **1997**, *B36*, 221.

(17) Caminiti, R.; Sadun, C.; Bionducci, M.; Buffa, F.; Ennas, G.; Licheri, G.; Musinu, A. *Gazz. Chim. Ital.* **1997**, *127*, 59.

(18) Caminiti, R.; Sadun, C.; Rossi, V.; Cilloco, F.; Felici, R. Presented at the XXV National Congress of Physical Chemistry, Cagliari, Italy, June 17–21, 1991; Pat. Appl. 01261484, June 23, 1993.

(19) Caminiti, R.; Gleria, M.; Lipkowitz, K. B.; Lombardo, G. M.; Pappalardo, G. C. *J. Am. Chem. Soc.* **1997**, *119*, 2196.

(20) Larson, A. C.; Von Dreele, R. B. *GSAS General Structure Analysis System*, LAUR 86-748; Los Alamos National Laboratory: Los Alamos, NM, 1985.

(21) Baerlocher, Ch. Restraints and constraints in Rietveld refinement. In *The Rietveld method*; Young, R. A., Ed.; Oxford Science Publications: New York, 1993.

(22) Howard, C. J. *J. Appl. Crystallogr.* **1982**, *15*, 615.

(23) Young, R. A., Ed. *The Rietveld method*. Oxford Science Publications: New York, 1993.

(24) Bunge, H.-J. *Texture Analysis in Materials Science*; Butterworth: London, 1982.

(25) Von Dreele, R. B. *J. Appl. Crystallogr.* **1997**, *30*, 517.

The structure of the  $\alpha$  phase of PcCo has been in the past the object of many structure investigations that always led to qualitative results due to the lack of suitable single crystals. A few hypotheses about the metric and the symmetry of the unit cell were proposed in the past.<sup>9,10</sup> However, it must be pointed out that the fiber diagram and the Debye photograph of the two references cited above showed very different values of the interplanar spacings and related intensities (Table 1), despite the similarity of the reported cell parameters (ref 9,  $a = 25.88$  Å,  $b = 3.750$  Å,  $c = 24.08$  Å,  $\beta = 90.2^\circ$ , space group  $C2/c$ ; ref 10,  $a = 25.4(1)$  Å,  $b = 3.77(2)$  Å,  $c = 24.6(1)$  Å, space group  $C2/c$ , if  $\beta \approx 90^\circ$ , or  $Ccc2$ , if  $\beta = 90^\circ$ ). In particular, whereas the data referring to the vacuum sublimed sample<sup>9</sup> clearly indicated the similarity among the  $\alpha$  forms of PcFe, PcH<sub>2</sub>, and PcCo, those of the acid paste sample<sup>10</sup> seemed to be consistent with a different phase. Our present data are consistent with those for the previous sample of  $\alpha$ -PcCo, prepared identically.

According to these facts, we started our structural study on the  $\alpha$ -form of PcCo using as reference the recent structural data of the  $\alpha$ -form of the metal-free phthalocyanine.<sup>6</sup> Starting unit cell parameters were  $a = 26.124(3)$  Å,  $b = 3.801(1)$  Å,  $c = 23.889(3)$  Å,  $\beta = 94.18(2)^\circ$ ,  $Z = 4$ , and space group  $C2/n$ : the only obvious modification with respect to the metal-free structure was the insertion at the origin of the Co atom. The refinement strategy was the same adopted for the  $\beta$  form; however, despite the relevant number of attempts, we were not able to obtain a satisfactory fit between the experimental and calculated patterns. A further attempt was carried out, on the basis of the strong relationships existing between our powder diffraction pattern and those of  $\alpha$ Ia Cu phthalocyanine and  $\alpha$ Ia 4-monochlororo Cu phthalocyanine,<sup>26</sup> which were assigned a triclinic symmetry with cell parameters  $a = 12.2$  Å,  $b = 3.74$  Å,  $c = 13.2$  Å,  $\alpha = 90^\circ$ ,  $\beta = 90.7^\circ$ ,  $\gamma = 95.6^\circ$ , and  $Z = 1$ . It should be also noticed that our powder spectrum bears strong resemblance with that of  $\alpha$ -PcZn.<sup>27,28</sup>

High-resolution transmission electron microscopy (HRTEM) images of vacuum-deposited  $\alpha$ -PcZn<sup>7</sup> indicate the presence of various polymorphs. Among them, the  $\alpha$ I form was characterized by periodicities of 13 and 12 Å in the direction of the  $a$  and  $c$  axis with an angle between the two axes of  $93^\circ$ . The authors, however, doubled the cell parameters in both directions in order to make them coincide with the unit-cell dimensions of the  $\alpha$ -PcPt.<sup>5</sup> A close inspection of Figure 4 of ref 7 clearly reveals that each PcZn molecule repeats itself, in effect, every 13 and 12 Å. This multiple cell was subsequently used to index the powder spectra of  $\alpha$ -PcZn.

According to these data we derived the positional parameters of a molecule of PcCo with the Co atom located at the origin. This was simply derived by inversion of the  $a$  and  $c$  axes and doubling the  $x$  and  $z$  positional parameters of the  $\alpha$ -form of the metal-free phthalocyanine.<sup>6</sup> Isotropic thermal parameters were fixed to the values corresponding to those of the single crystal work on  $\beta$ -PcCo.<sup>3</sup>

The refinement was carried out in  $P1$ , with the same procedure described above for the  $\beta$  form of the Co phthalocyanine. Immediately it became apparent that the starting structure was substantially correct, as the calculated diffraction pattern showed peak positions and intensities comparable with the experimental pattern. The refinement was limited to the  $5.5$ – $50^\circ$   $2\theta$  angular range because of the strong intensity decaying for  $2\theta$  angles  $> 50^\circ$ . As in the case of  $\beta$ -PcCo, hydrogen atoms were included to the refinement in positions derived from geometrical calculations and refined using the same set of soft constraints on bond distances and angles used for  $\beta$ -PcCo. A careful scrutiny of the residuals indicates the presence of some degree of preferred orientation [ $\bar{2}10$ ] that was initially modeled using the March–Dollase approach.<sup>29</sup> The corresponding coefficient refined to  $0.890(5)$ , and convergence was reached at  $R_p = 0.067$ ,  $wR_p = 0.089$ ,  $\chi^2 = 2.47$ , and  $R_{BRAGG} = 0.108$ . Alternatively the spherical-harmonic description was applied (the maximum order was set equal to four): a texture index  $J = 8.68$  was obtained and a significant improvement of the quality of the fitting was reached as indicated by the agreement indices  $R_p =$

**Table 2.** Miscellaneous Data for the Rietveld Refinement of  $\alpha$ - and  $\beta$ -PcCo

	$\alpha$ -PcCo	$\beta$ -PcCo
space group	$P\bar{1}$	$P2_1/c$
$a$ (Å)	12.090(8)	14.5982(9)
$b$ (Å)	3.754(2)	4.7937(3)
$c$ (Å)	12.800(9)	19.4348(11)
$\alpha$ (deg)	88.96(6)	90
$\beta$ (deg)	90.97(6)	120.782(3)
$\gamma$ (deg)	95.09(7)	90
$V$ (Å <sup>3</sup> )	578.4(9)	1168.4(1)
$\rho_{\text{calc}}$ (g/cm <sup>3</sup> )	1.641	1.624
angular range ( $2\theta$ , deg)	5.5–50	11.5–90
$R_p$	0.055	0.067
$wR_p$	0.075	0.089
$R_{BRAGG}$	0.133	0.121
reduced $\chi^2$	1.74	1.45
soft constr contribution to $\chi^2$ (%)	1.8	1.9
refined params	113	119
texture index	8.68	1.51
profile params		
GW	0	2.9(6)
LX	58(1)	3.9(3)
LY	44(6)	21(1)
asym	0	3.44(7)

0.055,  $wR_p = 0.075$ , and  $R_{\text{EXP}} = 0.058$ . Miscellaneous data of the refinement of  $\alpha$  and  $\beta$  forms are reported in Table 2, and final positional parameters and isotropic thermal parameters, in Table 3a,b. Experimental, calculated, and difference plots of the refinement are shown in Figure 2.

### Structure Descriptions

The refined structure of  $\beta$  Co phthalocyanine is in close agreement with reference data<sup>3,11</sup> and is very similar to that of  $\beta$  Mn, Fe, and Zn phthalocyanine<sup>1–4</sup> (Figure 3). The observed differences in bond lengths and angles of the molecule are extremely small.

The two independent Co–N bond distances are 1.907(4) and 1.910(4) Å: these values are extremely close to those of reference data<sup>3</sup> (1.906(2) and 1.909(2) Å). The mean C–N bond distance in the 16-membered ring around the Co atom is 1.347 Å, but it is 1.316(4) Å for the nitrogen atoms interconnecting the isoindole rings and 1.387(7) Å for those pertaining to the rings. These values compare well with those of the previously refined structure of  $\beta$ -PcCo<sup>3</sup> (1.317 and 1.375 Å, respectively) and are close to those observed in  $\beta$  Mn<sup>1,3</sup> (ref 1, 1.323 and 1.388 Å; ref 3, 1.316 and 1.394 Å), Fe<sup>1</sup> (1.322 and 1.378 Å), Zn<sup>2</sup> (ref 2, 1.331 and 1.369 Å), and metal-free<sup>4</sup> (1.326 and 1.374 Å) phthalocyanines. The two crystallographically independent phenyl rings show a mean C–C bond distance of 1.391(3) Å. As a general remark it must be remembered that the standard deviations of the Rietveld refinements are optimistic, because of the presence of local correlations,<sup>30</sup> and affected by the statistical weight imposed to the soft-constraints (for the contributions of the soft constraints to  $\chi^2$ , see Table 2). In the case of the present refinement inspection of the normal probability plot indicates that the residuals are normally distributed, as indicated by a slope of 1.17 and an intercept of 0.071.

A comparison between our and reference structural data<sup>3</sup> confirms the accuracy and precision of Rietveld analysis.<sup>31</sup> In particular the mean differences  $\Delta$  of the  $x$ ,  $y$ , and  $z$  coordinates of non-hydrogen atoms of the two refinements are 0.0035, 0.0087, and 0.0021, respectively, to be compared to average standard deviations  $\sigma$  of 0.0009, 0.0040, and 0.0008. According

(26) Honigmann, B.; Lenné, H.-U.; Schrödel, R. *Z. Krist.* **1965**, *122*, 185.

(27) Kobayashi, T.; Uyeda, N.; Suito, E. *J. Phys. Chem.* **1968**, *72*, 2446.

(28) Iwatsu, F.; Kobayashi, T.; Uyeda, N. *J. Phys. Chem.* **1980**, *84*, 3223.

(29) Dollase, W. A. *J. Appl. Crystallogr.* **1986**, *19*, 267.

(30) Berar, J.-F.; Lelann, P. *J. Appl. Crystallogr.* **1991**, *24*, 1.

(31) Kaduk, J. A.; Partenheimer, W. *Powder Diffr.* **1997**, *12*, 27.

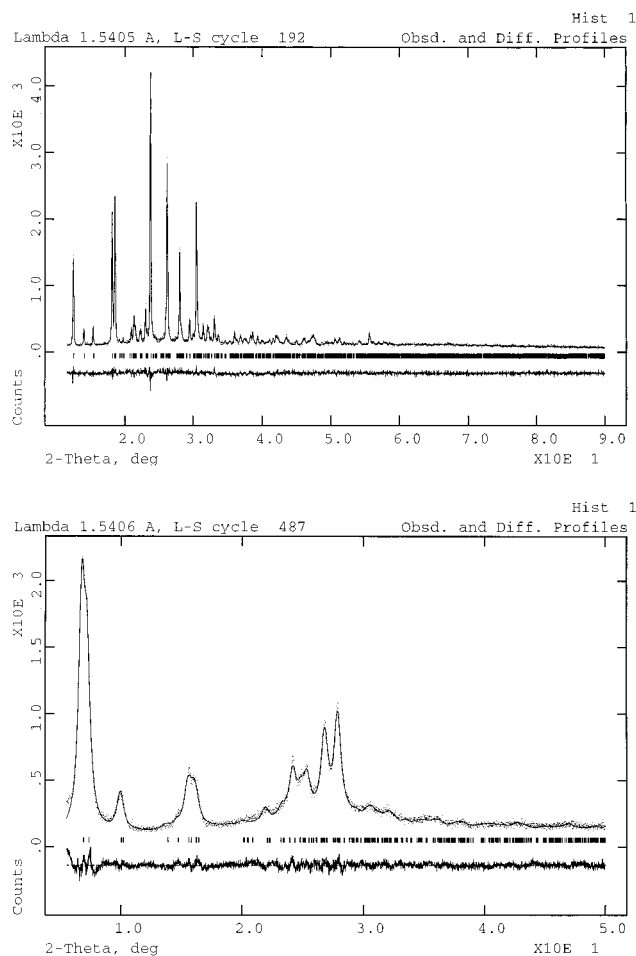


**Figure 2.** Observed, calculated, and difference powder diffraction patterns of (a, top)  $\beta$ - and (b, bottom)  $\alpha$ -PcCo. Vertical marks refer to the position of all possible reflections.

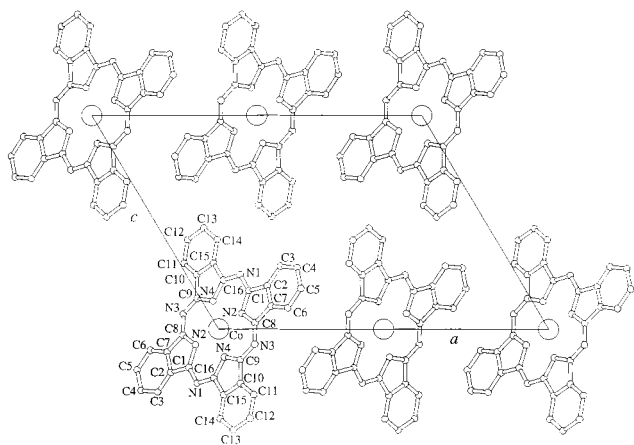


**Figure 3.** Molecular arrangement and atomic numbering scheme of  $\beta$ -PcCo as seen along [010]. For the sake of clarity a unit cell has been indicated.

to these figures the  $\Delta/\sigma$  ratio has an average value of 2.9. The average difference of the bond distances is constantly  $\leq \sigma$  (Table 4).

As previously indicated, two different refinements were carried out on  $\alpha$ -PcCo depending on the model (March–Dollase or generalized spherical-harmonic) used for the description of the effect of texture on reflection intensities. Differences between the positional parameters derived from the application of the

**Table 3.** Final Positional Parameters and Isotropic Thermal Parameters of Non-Hydrogen Atoms of  $\alpha$ - and  $\beta$ -PcCo

atoms	<i>x</i>	<i>y</i>	<i>z</i>	<i>B</i>
$\alpha$ -PcCo				
Co	0	0	0	2.0 <sup>a</sup>
N1	0.2476(18)	0.361(14)	0.0850(14)	2.6
N2	0.0645(14)	0.113(12)	0.1339(7)	2.6
N3	-0.0912(22)	-0.033(17)	0.2476(12)	2.6
N4	-0.1395(15)	-0.133(16)	0.0640(11)	2.6
C1	0.1611(22)	0.336(11)	0.1470(16)	2.6
C2	0.1683(22)	0.460(10)	0.2541(17)	2.6
C3	0.2523(24)	0.658(12)	0.3095(25)	2.6
C4	0.2589(33)	0.626(16)	0.4179(26)	2.6
C5	0.1988(27)	0.335(18)	0.4656(21)	2.6
C6	0.1029(32)	0.185(19)	0.4153(15)	2.6
C7	0.0868(21)	0.250(14)	0.3091(11)	2.6
C8	0.0144(18)	0.074(12)	0.2305(10)	2.6
C9	-0.1583(28)	-0.151(18)	0.1706(10)	2.6
C10	-0.2673(27)	-0.332(15)	0.1892(12)	2.6
C11	-0.3250(33)	-0.439(15)	0.2792(14)	2.6
C12	-0.4261(33)	-0.647(16)	0.2711(20)	2.6
C13	-0.4625(25)	-0.783(14)	0.1749(22)	2.6
C14	-0.3965(32)	-0.713(12)	0.0874(17)	2.6
C15	-0.3084(26)	-0.449(12)	0.0923(12)	2.6
C16	-0.2365(15)	-0.268(10)	0.0143(10)	2.6
$\beta$ -PcCo <sup>b</sup>				
Co	0	0	0	4.6(3)
	0	0	0	1.95(2)
N1	0.2482(7)	0.030(4)	0.1596(7)	3.8(2) <sup>c</sup>
	<i>0.2514(2)</i>	<i>0.0268(6)</i>	<i>0.1597(1)</i>	<i>2.1(1)</i>
N2	0.0677(7)	0.213(3)	0.0965(6)	3.8(2)
	<i>0.0718(2)</i>	<i>0.2178(5)</i>	<i>0.0960(1)</i>	<i>2.1(1)</i>
N3	-0.0744(8)	0.528(3)	0.0744(8)	3.8(2)
	<i>-0.0721(2)</i>	<i>0.5168(7)</i>	<i>0.0785(1)</i>	<i>2.5(1)</i>
N4	-0.1331(5)	0.168(3)	-0.0276(7)	3.8(2)
	<i>-0.1307(2)</i>	<i>0.1947(6)</i>	<i>-0.0326(1)</i>	<i>2.1(1)</i>
C1	0.1736(9)	0.194(4)	0.1566(9)	3.8(2)
	<i>0.1779(2)</i>	<i>0.1957(6)</i>	<i>0.1569(2)</i>	<i>2.1(1)</i>
C2	0.1955(8)	0.403(4)	0.2170(8)	3.8(2)
	<i>0.1998(2)</i>	<i>0.3936(6)</i>	<i>0.2205(2)</i>	<i>2.4(1)</i>
C3	0.2836(10)	0.456(5)	0.2923(9)	3.8(2)
	<i>0.2906(2)</i>	<i>0.4498(7)</i>	<i>0.2924(2)</i>	<i>2.8(1)</i>
C4	0.2765(10)	0.654(4)	0.3420(8)	3.8(2)
	<i>0.2821(3)</i>	<i>0.6519(8)</i>	<i>0.3415(2)</i>	<i>3.2(1)</i>
C5	0.1834(13)	0.807(4)	0.3149(9)	3.8(2)
	<i>0.1875(3)</i>	<i>0.7954(8)</i>	<i>0.3174(2)</i>	<i>3.4(1)</i>
C6	0.0955(11)	0.756(4)	0.2393(10)	3.8(2)
	<i>0.0970(2)</i>	<i>0.7406(7)</i>	<i>0.2438(2)</i>	<i>2.9(1)</i>
C7	0.0987(7)	0.533(4)	0.1944(8)	3.8(2)
	<i>0.1055(2)</i>	<i>0.5373(7)</i>	<i>0.1963(2)</i>	<i>2.3(1)</i>
C8	0.0232(9)	0.430(4)	0.1153(8)	3.8(2)
	<i>0.0273(2)</i>	<i>0.4243(6)</i>	<i>0.1185(2)</i>	<i>2.3(1)</i>
C9	-0.1457(8)	0.389(4)	0.0115(9)	3.8(2)
	<i>-0.1444(2)</i>	<i>0.4048(6)</i>	<i>0.0095(2)</i>	<i>2.2(1)</i>
C10	-0.2564(8)	0.476(4)	-0.0309(8)	3.8(2)
	<i>-0.2551(2)</i>	<i>0.4957(8)</i>	<i>-0.0325(2)</i>	<i>2.4(1)</i>
C11	-0.3114(11)	0.683(4)	-0.0166(11)	3.8(2)
	<i>-0.3080(2)</i>	<i>0.6942(7)</i>	<i>-0.0134(2)</i>	<i>2.9(1)</i>
C12	-0.4193(10)	0.721(4)	-0.0705(11)	3.8(2)
	<i>-0.4164(3)</i>	<i>0.7274(8)</i>	<i>-0.0667(2)</i>	<i>3.5(1)</i>
C13	-0.4727(8)	0.542(4)	-0.1353(9)	3.8(2)
	<i>-0.4693(2)</i>	<i>0.5660(7)</i>	<i>-0.1358(2)</i>	<i>3.2(1)</i>
C14	-0.4193(10)	0.368(5)	-0.1561(9)	3.8(2)
	<i>-0.4168(2)</i>	<i>0.3688(7)</i>	<i>-0.1551(2)</i>	<i>2.8(1)</i>
C15	-0.3054(8)	0.337(4)	-0.1042(8)	3.8(2)
	<i>-0.3081(2)</i>	<i>0.3358(6)</i>	<i>-0.1016(2)</i>	<i>2.4(1)</i>
C16	-0.2253(10)	0.153(4)	-0.1023(8)	3.8(2)
	<i>-0.2287(2)</i>	<i>0.1507(6)</i>	<i>-0.1012(2)</i>	<i>2.2(1)</i>

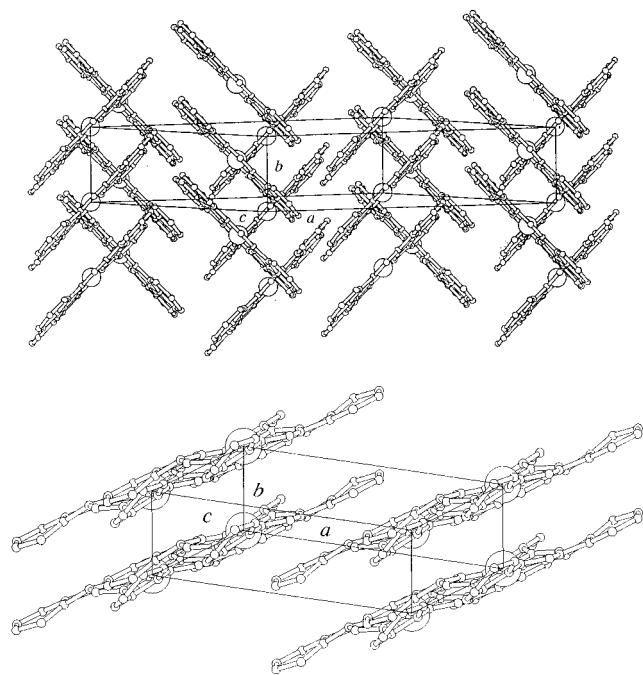
<sup>a</sup> Values taken from the single-crystal reference data. They were kept fixed during the refinement. <sup>b</sup> For comparison the data of Mason et al. (1979) are also reported in italics. <sup>c</sup> Value constrained to be equal for all the non-Co atoms.

two models were observed, corresponding to a mean  $\Delta/\sigma$  ratio value of 4.9. In particular whereas the differences on the *x* and

**Table 4.** Bond Distances (Å) of  $\alpha$ - and  $\beta$ -PcCo<sup>a</sup>

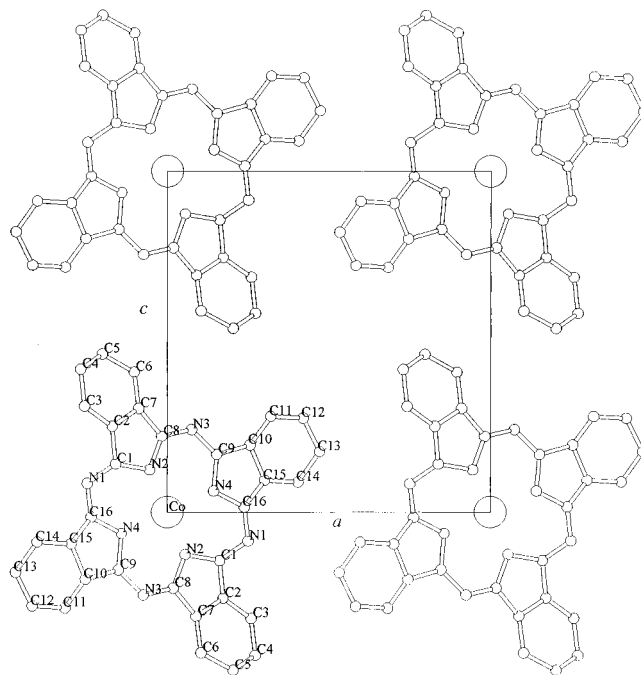
Co–N2	1.910(5)	C3–C4	1.393(7)		
Co–N4	1.909(5)	C4–C5	1.394(7)		
N1–C1	1.320(7)	C5–C6	1.396(7)		
N1–C16	1.325(7)	C6–C7	1.390(7)		
N2–C1	1.384(7)	C7–C8	1.452(7)		
N2–C8	1.386(7)	C9–C10	1.450(7)		
N3–C8	1.324(7)	C10–C11	1.391(6)		
N3–C9	1.324(6)	C10–C15	1.392(7)		
N4–C9	1.387(7)	C11–C12	1.393(7)		
N4–C16	1.386(7)	C12–C13	1.390(7)		
C1–C2	1.454(7)	C13–C14	1.394(7)		
C2–C3	1.395(6)	C14–C15	1.390(7)		
C2–C7	1.398(7)	C15–C16	1.453(7)		
	present work	Mason et al. (1979)	present work	Mason et al. (1979)	
Co–N2	1.907(4)	1.906(2)	C3–C4	1.395(6)	1.378(5)
Co–N4	1.910(4)	1.909(2)	C4–C5	1.390(6)	1.386(5)
N1–C1	1.320(5)	1.318(4)	C5–C6	1.392(6)	1.381(4)
N1–C16	1.321(6)	1.313(4)	C6–C7	1.394(6)	1.384(5)
N2–C1	1.384(6)	1.385(3)	C7–C8	1.446(6)	1.448(3)
N2–C8	1.372(6)	1.368(4)	C9–C10	1.449(5)	1.449(4)
N3–C8	1.313(6)	1.318(4)	C10–C11	1.392(6)	1.383(5)
N3–C9	1.310(6)	1.318(3)	C10–C15	1.394(6)	1.385(4)
N4–C9	1.371(6)	1.369(4)	C11–C12	1.387(6)	1.381(4)
N4–C16	1.386(6)	1.378(3)	C12–C13	1.387(6)	1.385(5)
C1–C2	1.450(6)	1.451(4)	C13–C14	1.391(6)	1.379(6)
C2–C3	1.390(6)	1.386(3)	C14–C15	1.389(6)	1.385(4)
C2–C7	1.393(6)	1.383(4)	C15–C16	1.449(5)	1.452(5)

<sup>a</sup> For  $\beta$ -PcCo the Data of Mason et al. (1979) are also reported.

**Figure 4.** Mutual arrangement of the layers of molecules in (a, top)  $\beta$  and (b, bottom)  $\alpha$ -PcCo.

$y$  coordinates are relatively small ( $\langle \Delta/\sigma \rangle = 3.2$ ) more pronounced discrepancies were found for the  $z$  coordinates ( $\Delta/\sigma = 8.3$ ). We will discuss here the molecular arrangement obtained through the generalized spherical-harmonic description of texture as it represents the best fitting of our experimental data.

The  $\alpha$  form of the Co phthalocyanine has a different stacking of the molecules with respect to  $\beta$ -PcCo: in fact whereas in the  $\beta$  form the adjacent columns of molecules are almost perpendicular, in the  $\alpha$  form they are parallel (Figure 4a,b). This arrangement is also different with respect to the  $\alpha$  form of the metal-free<sup>6</sup> and Pt phthalocyanine,<sup>5</sup> where the angle is ca. 125°.

**Figure 5.** Molecular arrangement and atomic numbering scheme of  $\alpha$ -PcCo as seen along [010]. For the sake of clarity a unit cell has been indicated.

The molecular packing of  $\alpha$ -PcCo results in a unit cell that contains only one macrocyclic unit (Figure 5). The geometry of the molecule does not show any significant difference with respect to the  $\beta$  form as indicated by the mean C–N bond distance in the 16-membered ring of 1.354 Å, of 1.323(2) Å for the N atoms located between the isoindole rings, and 1.386–(1) Å for those pertaining to the rings. The two independent phenyl rings show a mean C–C bond distance of 1.393(6) Å. The angle between the  $b$  axis and the normal of the mean plane of the molecule is ca. 30°.

As in the case of  $\beta$ -PcCo the residuals are normally distributed, as indicated by a slope of 1.24 and an intercept of 0.047 of the normal probability plot.

The standard deviations of the cell parameters of the  $\alpha$  form are almost of 1 order of magnitude higher than those of the  $\beta$  form. This is due to the difficulty to locate the centroid of the peaks because of their extremely large full-width at half maximum (FWHM). The coefficients of the powder profile may be, however, related to the crystallite size. From the profile-function parameter LX it is in effect possible to obtain the average particle size  $p(\text{Å})$ .<sup>20</sup> A refined isotropic value of 152 Å was therefore obtained indicating a particle size of the same order of magnitude of nanocompounds. This value compares very favorably with the crystallite size of vacuum-sublimated  $\alpha$ -PcZn (147 Å) as determined from powder diffraction.<sup>28</sup>

### $\alpha \rightarrow \beta$ Phase Transition

**I. EDXD Data.** Data on the kinetics of the isothermal  $\alpha \rightarrow \beta$  phase transition of phthalocyanines have been reported in the past.<sup>32,33</sup> It has been pointed out<sup>8</sup> that the rate of the phase transition depends mainly on the temperature and that in a vacuum the rate is faster and takes place at a lower temperature than in atmosphere. Moreover, a significant effect on the rate of reaction of the type of the central M atom has been observed.

(32) Sharp, J. H.; Miller, R. L. *J. Phys. Chem.* **1968**, *72*, 3335.

(33) Kawashima, N.; Suzuki, T.; Meguro, K. *Bull. Chem. Soc. Jpn.* **1976**, *49*, 2029.

These variables account for the large thermal range (ca. 150–ca. 350 °C) which has been investigated in the past. In particular IR data were used to obtain the first-order rate constant of metal-free phthalocyanine.<sup>32</sup> From the Arrhenius plot the authors derived an activation enthalpy of 31.2(4) kcal/mol. This value has been obtained from data sets collected at 5 different temperatures in the range 260–343 °C. However, according to the structural determination of the present study on  $\alpha$ -PcCo and that of  $\alpha$ -PcH<sub>2</sub><sup>6</sup> it is clear that the two compounds are not isostructural.

A significantly lower value was obtained on a subsequent work<sup>33</sup> for  $\alpha$  PcCu suspended in organic solvents (*p*-xylene). In fact, on the basis of the X-ray powder diffraction experiments, the authors calculated a value of 17.6 kcal/mol. In this case, according to the reported powder diffraction pattern and that found in a previous work,<sup>26</sup> isostructurality between  $\alpha$ -PcCo and  $\alpha$ -PcCu may be assumed.

In the present work the isothermal  $\alpha \rightarrow \beta$  phase transition of PcCo has been followed in-situ real-time by means of EDXD<sup>15–17</sup> and DSC.

The EDXD experiments were carried out in reflection-mode on a pellet prepared by pressing the powder of the  $\alpha$  phase. Three different temperatures were chosen for the investigation: 152, 250, and 300 °C. The temperature of 152 °C was selected because it represents the monotropic, thermal-transition temperature of pure zinc phthalocyanine,<sup>27</sup> whereas the value of 300 °C was chosen because, following reference data,<sup>34</sup> it represents the  $\alpha \rightarrow \beta$ -PcCo transition temperature. However, at this temperature, the transition was found to be so fast that it was completed at the end of the fourth frame (640 s). This fact indicated that it is probable that much of the transition had occurred while the sample was heating from room temperature to 300 °C. For this reason the whole data set was discarded. A further experiment was carried out also at 250 °C: in this case the reaction proceeded at a significantly slower pace than at 300 °C.

The phase transition has been qualitatively described by plotting the fraction of the  $\beta$  phase  $X(t)$  vs time. As a starting assumption, we considered every intermediate spectrum  $I_t$  as a linear combination of the two extreme ones. The values of  $X(t)$  have been therefore evaluated from the equation

$$X(t) = \frac{(I_t - I_{in})}{(I_{fin} - I_{in})} \quad (2)$$

where  $I_{in}$  is the intensity scattered by the sample in its initial state ( $\alpha$ -PcCo) and  $I_{fin}$  that in its final state ( $\beta$ -PcCo).

The  $\alpha$ -PcCo and  $\beta$ -PcCo EDXD spectra are reported in Figure 6. The spectrum of  $\alpha$ -PcCo shows three broad peaks located at  $q \sim 0.5, 0.7,$  and  $1.1 \text{ \AA}^{-1}$ , whereas that of  $\beta$  Co phthalocyanine is considerably more complex showing five sharper peaks located at  $\sim 0.5, 0.7, 0.75, 0.9,$  and  $1.3 \text{ \AA}^{-1}$  (see Table 5 for the indexing).

Each diffraction pattern has been divided into five different zones ( $0.42\text{--}0.56, 0.56\text{--}0.69, 0.82\text{--}0.92, 0.92\text{--}1.16,$  and  $1.16\text{--}1.36 \text{ \AA}^{-1}$ ) where the intensities have been separately integrated. This has been done in order to observe the decreasing and increasing of intensity of the various clusters of peaks. The two ranges,  $0.82\text{--}0.92,$  and  $1.16\text{--}1.36 \text{ \AA}^{-1}$ , are particularly interesting in that each one contains only reflections of the  $\beta$  form (one and three peaks, respectively) whereas all the other ranges contain peaks of both polymorphs. The assumption was made of a constant bulk density of the sample throughout the

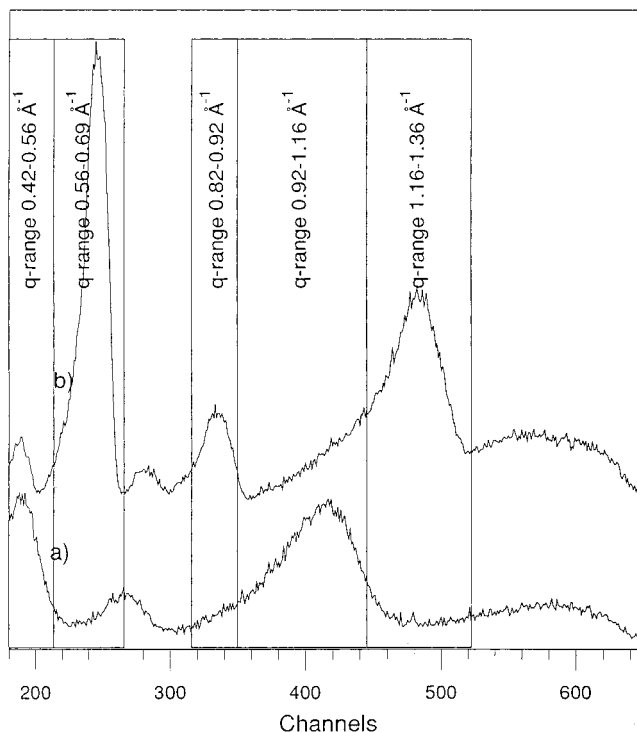


**Figure 6.** (a) Initial EDXD spectrum of the bulk material ( $\alpha$ -PcCo). (b) Final EDXD spectrum after isothermal heating ( $\beta$ -PcCo). Integration ranges are also indicated. Data were collected at a diffraction angle of  $2.2^\circ$  in  $2\theta$ .

transformation, in agreement with the two calculated densities of  $1.641$  ( $\alpha$ -form) and  $1.624$  ( $\beta$ -form)  $\text{g/cm}^3$  (difference  $\sim 1.0\%$ ). No deformation of the pellet was detected after the thermal process.

As a first remark two different behaviors have been observed: in particular the first two ranges ( $0.42\text{--}0.56, 0.56\text{--}0.69 \text{ \AA}^{-1}$ ) show a rate of reaction significantly lower than that of the other three ranges. This is clearly indicated by the time needed for reaching the 50% of the reaction ( $X(t) = 0.5$ ) which is (by interpolation) of 500 s (first two ranges) and 100 sec (other three ranges), respectively, at 250 °C (Figure 7).

The same results have been obtained during the isothermal study at 152 °C. Obviously the kinetic at this temperature is extremely sluggish and the completeness of the phase transition was not reached even after 3.5 days. However, the same behavior of two rates of reaction has been observed.

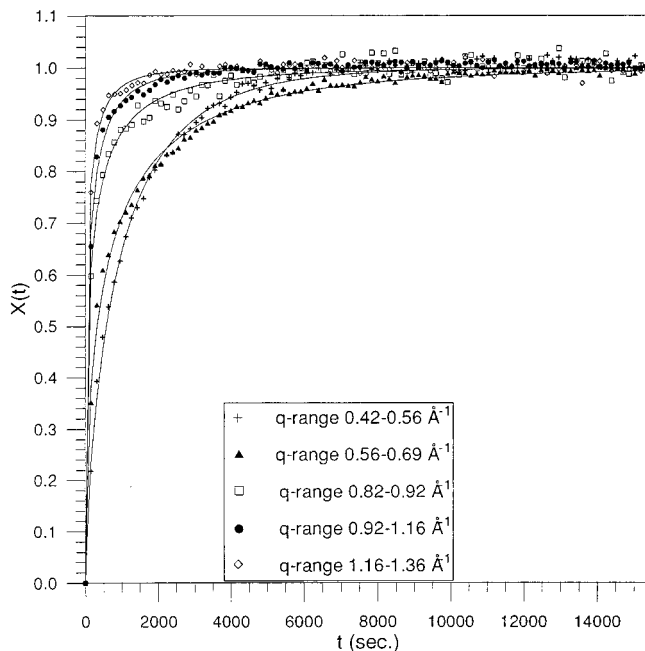
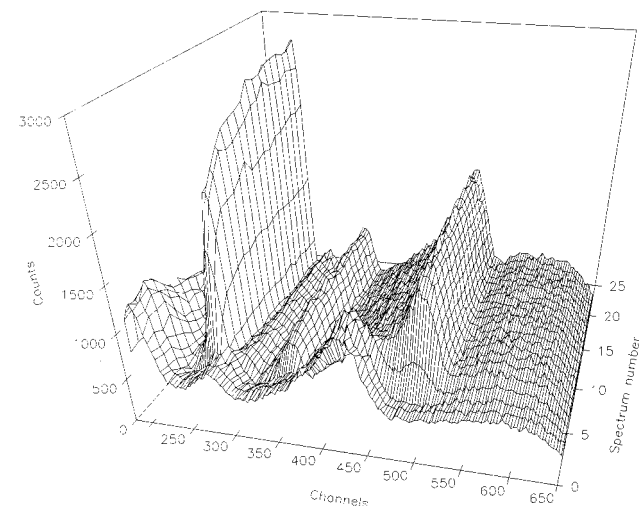
From a careful scrutiny of the EDXD spectra some additional information has been extracted. In particular it is clear that the peaks corresponding to the  $\alpha$ -form disappear almost immediately and, concomitantly, those attributed to the  $\beta$ -form start to grow. We were not able to detect any preliminary growth of the  $\alpha$ -form crystallites before transformation into the  $\beta$ -form, different from the reported behavior of PcCu.<sup>33,35</sup> In fact the FWHM of the peaks of the  $\alpha$ -form was constant throughout the transformation process. However, after the peaks of the  $\alpha$ -form have completely disappeared, those of the  $\beta$ -form continue to increase in intensity (Figure 8). This is not an effect of a crystal-growth process of the  $\beta$ -form, because in this case only the height of the peaks will increase but not the corresponding integrated intensity. Only in the final stage of the reaction the peaks sharpen indicating a crystal growth process. According to these data, we propose the following three steps model for the  $\alpha \rightarrow \beta$ -PcCo phase transition that takes place at 152 and 250 °C: (1) There is

(34) Assour, J. M.; Kahn, W. K. *J. Am. Chem. Soc.* **1965**, *87*, 207.

(35) Suito, E.; Uyeda, N. *Kolloid Z.* **1963**, *193*, 97.

**Table 5.** Integration Ranges and Peak Reflections Located within

	q range ( $\text{\AA}^{-1}$ )				
	0.42–0.56	0.56–0.69	0.82–0.92	0.92–1.16	1.16–1.36
$\alpha$ -form	(001) vs, (100) vs	(10 $\bar{1}$ ) s, (101) s	(002) w, (200) w, (10 $\bar{2}$ ) w, (102) s, (201) s, (201) w		
$\beta$ -form	(001) vs	(20 $\bar{1}$ ) s	(202) m	(002) w, (201) w	(20 $\bar{3}$ ) m, (40 $\bar{2}$ ) w, (40 $\bar{1}$ ) m

**Figure 7.** Data for the fraction  $X(t)$  of  $\beta$ -PcCo formed during the  $\alpha \rightarrow \beta$  phase transition at 250 °C. The plots refers to the five different  $q$ -ranges (see text for explanation).**Figure 8.** Three-dimensional plots channels–intensity–time of the  $\alpha \rightarrow \beta$  phase transition collected at 250 °C.

disordering of adjacent columns of molecules of phthalocyanine from their original  $\alpha$ -type arrangement (on the EDXD spectra this step corresponds to the decreasing of the intensities of the peaks of the  $\alpha$ -form). (2) There is crystallization of the  $\beta$ -form from the disordered phase by rearrangement of the columns of Pc molecules. No evidence of the occurrence of intermediate ordered phases ( $\gamma$  form of  $\text{ZnPc}^{28}$ ) was observed (the peaks of the  $\beta$ -form become apparent). (3) Finally, there is crystal growth of the  $\beta$ -phase from ingestion of various nuclei to an average particle size of 2500  $\text{\AA}$ , as indicated by the fitted peak-profile

**Table 6.** Fitting Parameters of the Avrami Equation for the Isothermal DSC Data<sup>a</sup>

temp (°C)	$t_{in}$ (s)	$1/T$ (K)	$n$	$k$ (s) <sup>-1</sup>	$\ln k$	$R^2$
270	20	$1.841 \times 10^{-3}$	2.34(7)	0.359(3)	-1.024	0.996
267.5	31	$1.850 \times 10^{-3}$	2.42(5)	0.328(2)	-1.114	0.998
265	29	$1.858 \times 10^{-3}$	2.40(5)	0.374(2)	-0.985	0.998
262.5	37	$1.867 \times 10^{-3}$	2.44(5)	0.327(2)	-1.119	0.998
260	46	$1.876 \times 10^{-3}$	2.54(5)	0.256(2)	-1.361	0.997
255	53	$1.893 \times 10^{-3}$	2.36(4)	0.274(1)	-1.295	0.998
250	68	$1.911 \times 10^{-3}$	2.68(5)	0.1807(9)	-1.711	0.997
245	87	$1.930 \times 10^{-3}$	2.52(7)	0.170(1)	-1.773	0.997
240	124	$1.949 \times 10^{-3}$	2.58(6)	0.1457(9)	-1.926	0.997
235	136	$1.968 \times 10^{-3}$	2.51(5)	0.1347(7)	-2.005	0.998
230	125	$1.987 \times 10^{-3}$	2.36(4)	0.1328(7)	-2.019	0.998
225	248	$2.007 \times 10^{-3}$	2.52(9)	0.108(1)	-2.228	0.996
220	314	$2.028 \times 10^{-3}$	2.49(8)	$9.57(9) \times 10^{-2}$	-2.347	0.997
215	559	$2.049 \times 10^{-3}$	2.51(5)	$6.67(3) \times 10^{-2}$	-2.708	0.997
210	855	$2.070 \times 10^{-3}$	2.62(8)	$4.13(3) \times 10^{-2}$	-3.186	0.996
205	1309	$2.091 \times 10^{-3}$	2.49(6)	$3.07(2) \times 10^{-2}$	-3.485	0.997
200	1970	$2.113 \times 10^{-3}$	2.45(8)	$2.19(2) \times 10^{-2}$	-3.823	0.998
195	3138	$2.136 \times 10^{-3}$	2.63(7)	$1.009(7) \times 10^{-2}$	-4.597	0.996
190	4406	$2.159 \times 10^{-3}$	2.46(7)	$8.64(7) \times 10^{-3}$	-4.751	0.996
182.5	8706	$2.195 \times 10^{-3}$	2.00(6)	$4.70(7) \times 10^{-3}$	-5.361	0.996

<sup>a</sup> See text for explanation of the symbols. Esd's are reported in parentheses.

parameters (increase of the intensities of the peaks of the  $\beta$ -form, coupled with a decreased FWHM).

**II. DSC Data.** The calorimetric data were collected over the range 182.5 °C <  $T$  < 270 °C (Table 6). Every isothermal run shows a well-defined single peak indicating a single-step  $\alpha \rightarrow \beta$  phase transition, without the occurrence of intermediate ordered phases.

Different from the EDXD data, an induction time of the isothermal phase transition has been observed. This delay is related to the temperature at which the experiment has been carried out, as indicated by the time  $t_{in}$  at which the phase transition starts. In particular different linear trends have been observed in the two ranges 225–270 and 182.5–225 °C in the  $1/T$  (K) vs  $\log(t_{in})$  plot (Figure 9). The data have been therefore used to derive the empirical activation energy  $E_a$  from this Arrhenius-like plot, following the procedure successfully applied in the kinetic analysis of the formation of zeolite L.<sup>36</sup> The values of 38.7(8) kcal/mol (temperature range: 182.5–225 °C) and 25.6(16) kcal/mol (temperature range: 225–270 °C) have been therefore derived.

The phase transition has been quantitatively analyzed by means of the Avrami equation<sup>37–39</sup> (eq 3), where  $X(t)$  represents

$$X(t) = 1 - \exp[-(kt)^n] \quad (3)$$

the fraction of the new phase at time  $t$  and  $k$  and  $n$  are constants. This equation assumes that a nucleation (assumed to be random) and growth mechanism characterize the transformation.

(36) Joshi, P. N.; Kotasthane, A. N.; Shiralkar, V. P. *Zeolites* **1990**, *10*, 598.

(37) Avrami, M. *J. Chem. Phys.* **1939**, *7*, 1103.

(38) Avrami, M. *J. Chem. Phys.* **1940**, *8*, 212.

(39) Avrami, M. *J. Chem. Phys.* **1941**, *9*, 177.



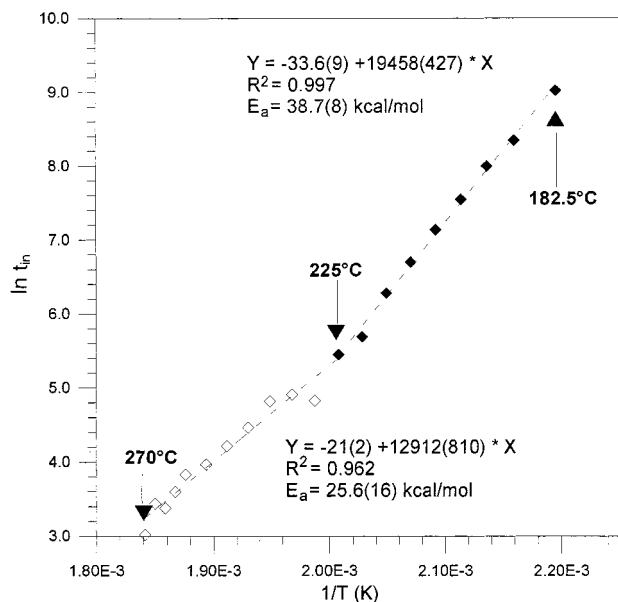


**Figure 9.** Arrhenius-like  $1/T$  (K) vs log induction time ( $t_{in}$ ) plot as determined from DSC data. The experimental points are aligned along two regression lines with significantly different slope.

The values of  $X(t)$  have been evaluated from the equation

$$X(t) = \frac{\int_{t_{in}}^t \frac{dQ}{dt} dt}{\int_{t_{in}}^{t_{fin}} \frac{dQ}{dt} dt} \quad (4)$$

where  $t_{in}$  is the time at which the process starts and  $t_{fin}$  is the time at which the process is completed. The  $t_{in}$  and  $t_{fin}$  values have been set, for each DSC run, as the minimum and the maximum of the first derivative of the peak, respectively. The  $X(t)$  vs  $t$  curves for the various isothermal phase transitions show the well-known sigmoid shape, indicating a typical autocatalytic process. Data were processed with local programs.

To numerically evaluate the sigmoid function a nonlinear fitting of the Avrami equation (number of data points ranging from 16 to 46) has been carried out.

The various DSC runs lead to a phenomenological  $n$  value comprised between 2.34 and 2.68, with the only exception of the data set collected at 182.5 °C characterized by an  $n$  value of 2.00. Therefore the phase transition should be described as isokinetic as the mechanism does not change within this temperature range. Furthermore the  $n$  values are indicative of a two-dimensional growth.

An estimate of the empirical activation energy  $E_a$  from an Arrhenius plot of  $\ln k$  against  $1/T$  has been also carried out. Since

$$k = A \exp\left(-\frac{E_a}{RT}\right) \quad (5)$$

this plot is linear with a slope of

$$-\frac{E_a}{RT}$$

As in the case of the induction time, two different linear trends have been observed into the two ranges 182.5–220 and 220–270 °C in the  $\ln k$  vs  $1/T$  plot (Figure 10). Correspondingly, two different values of the empirical activation energy  $E_a$  have been obtained for the two thermal ranges. These values are 36.6-

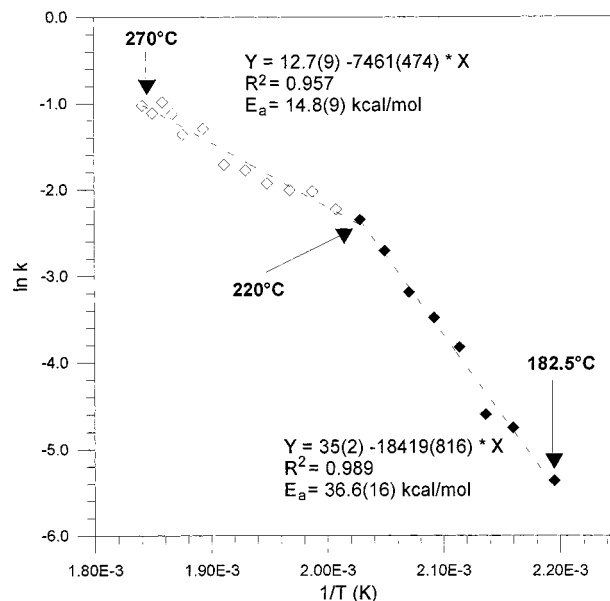


**Figure 10.** Arrhenius  $\ln k$  vs  $1/T$  plot for the DSC data in the range 182.5–270 °C. Two different behaviors, corresponding to two different empirical activation energies  $E_a$ , are evident.

(16) kcal/mol (temperature range: 182.5–220 °C) and 14.8(9) kcal/mol (temperature range: 220–270 °C). The empirical activation energy for the temperature range 182.5–220 °C compares favorably with the corresponding value as derived from the induction time (see above). A more pronounced discrepancy has been observed, on the contrary, for the temperature range 220–270 °C. Despite these differences, it is important to point out that in both cases a discontinuity has been detected in correspondence of almost the same temperature (220 and 225 °C). This discontinuity is therefore indicative of an abrupt change in both induction time and time necessary to complete the phase transition. The physical meaning of this change cannot be simply inferred. According to our expectation we may suspect that in the low-temperature range both nucleation and growth processes are present whereas at high temperature the prevailing process is that of nucleation. Following this reasoning we may hypothesize that 14.8(9) kcal/mol represents the energetical demand for the nucleation of  $\beta$ -PcCo.

As previously pointed out, the main difference between the two data set (EDXD and DSC) is that in EDXD no induction time has been observed (the intensity of the reflections changes immediately), whereas in DSC the transformation starts after a time that is related to the temperature at which the experiment has been carried out. This discrepancy may be due to the difficulty of DSC to detect small continuous distortions of the structure characterized by small thermal effects. These structural rearrangements, on the contrary, may significantly change the intensity of the EDXD reflections.

## Conclusions

The structure of the acid-paste  $\alpha$ -form of PcCo has been determined through the Rietveld method. This polymorph is characterized by a different way to stack the columns of molecules, which develops along the  $y$  direction with respect to  $\beta$ -PcCo. It is triclinic, space group  $P\bar{1}$ , cell parameters  $a = 12.090(8)$  Å,  $b = 3.754(2)$  Å,  $c = 12.800(9)$  Å,  $\alpha = 88.96(6)^\circ$ ,  $\beta = 90.97(6)^\circ$ ,  $\gamma = 95.09(7)^\circ$ , and  $Z = 1$ . Whereas in the  $\beta$  form adjacent columnar stacked molecules are perpendicularly aligned each other, leading to a zigzag array, in the  $\alpha$  form of

PcCo they are parallel. The arrangement is also different with respect to the  $\alpha$  form of the metal-free<sup>6</sup> and Pt phthalocyanine<sup>5</sup> where the angle is of ca. 125°. From the refined peak-profile parameters a crystallite size of  $\sim 150$  Å, value close to that of nanocompounds, has been estimated. Our structural data are in agreement with the HRTEM photograph of  $\alpha$ I PcZn<sup>7</sup> but not with the conclusions drawn by the referred authors. In particular our unit cell contains only one molecule with respect to the four indicated by ref 7. According to reference powder X-ray data<sup>9,10</sup> it is possible to hypothesize the presence of a further polymorph for PcCo: this polymorph could be possibly isostructural with  $\alpha$ -PcH<sub>2</sub> and  $\alpha$ -PcPt. The occurrence of this form could be related to the different preparation procedures referred above as (1) and (2).

The isothermal  $\alpha \rightarrow \beta$  phase transition has been followed in-situ real-time by means of EDXD. Two different data sets have been collected at 152 and 250 °C. Each diffraction pattern has been divided into five different zones where the intensities have been separately integrated. Two different behaviors have been observed: in particular the first two ranges, corresponding to long interplanar spacings, show a rate of reaction significantly lower than that of the other three ranges. This bimodality may be attributed to the higher or lower easiness to rearrange different types of interplanar spacings.

Calorimetric data were used to model the kinetics through the Avrami equation. Two different values of the empirical

activation energy  $E_a$  have been obtained from an Arrhenius plot of  $\ln k$  against  $1/T$ . These values are 36.6(16) kcal/mol (temperature range: 182.5–220 °C) and 14.8(9) kcal/mol (temperature range: 220–270 °C). An evaluation of the phenomenological  $n$  parameter indicates a 2D-growth mechanism. The phase transition may be described as isokinetic, at least in the investigated temperature range.

According to our results a three steps model for the  $\alpha \rightarrow \beta$ -PcCo phase transition has been proposed: (1) disordering of adjacent layers of molecules of phthalocyanine from its original  $\alpha$ -form; (2) crystallization of the  $\beta$ -form from this disordered phase through rearrangement of the layers of Pc molecules, where no evidence of the occurrence of intermediate ordered phases was observed; (3) 2D-crystal growth of the  $\beta$ -phase from the nuclei to an average particle size of 2500 Å, as indicated by the fitted peak-profile parameters.

**Acknowledgment.** Thanks are expressed to the Italian Research National Council (CNR) for financial support.

**Supporting Information Available:** Tables of additional bond lengths and hydrogen positional and thermal parameters (3 pages, print/PDF). See any current masthead page for ordering information and Internet access instructions.

JA973815P